

Hexadimethrine-montmorillonite nanocomposite: characterization and application as a pesticide adsorbent

B. Gámiz*, M.C. Hermosín, J. Cornejo, R. Celis

Instituto de Recursos Naturales y Agrobiología de Sevilla (IRNAS), CSIC, Avenida Reina Mercedes 10, P.O. Box 1052, 41080 Sevilla, Spain

*Corresponding author:

Dr. Beatriz Gámiz

Instituto de Recursos Naturales y Agrobiología de Sevilla (IRNAS), CSIC

Avenida Reina Mercedes 10, P.O. Box 1052

41080 Sevilla

SPAIN

Phone: +34 954624711

Fax: +34 954624002

E-mail: bgamiz@irnase.csic.es

Abstract

The goal of this work was to prepare and characterize a novel functional material by the modification of SAz-1 montmorillonite with the cationic polymer hexadimethrine (SA-HEXAD), and to explore the potential use of this nanocomposite as a pesticide adsorbent. Comparative preparation and characterization with the well-known hexadecyltrimethylammonium-modified SAz-1 montmorillonite (SA-HDTMA) was also assessed. The characterization was performed by elemental analysis, X-ray diffraction (XRD), Fourier-transform infrared spectroscopy (FTIR), physisorption of N₂, scanning electron microscopy (SEM) and Z potential measurements. The characterization and adsorption experiments showed that the extent of pesticide adsorption was markedly subjected to the structure and features of the surface of each organo-clay and also to the nature of the considered pesticide. SA-HEXAD displayed a high affinity for anionic pesticides which, presumably, were adsorbed by electrostatic attraction on positively-charged ammonium groups of the polymer not directly interacting with the clay. In contrast, SA-HDTMA displayed great adsorption of both uncharged and anionic pesticides with predominance of hydrophobic interactions. This work provided information about the surface properties of a new organic-inorganic nanohybrid material, SA-HEXAD, and its potential as an adsorbent for the removal of anionic organic pollutants from aqueous solutions.

Keywords: Adsorption; Functionalization; Nanostructured materials; Nanohybrids; Polymers

1. Introduction

Clay minerals have attracted attention over the last decades for being naturally occurring and versatile materials. The importance of these materials lies on their peculiar properties such as small particle size, swelling capacity, anisotropic shape, reactive surfaces, and high cation exchange capacity (CEC) [1,2]. As a consequence, a vast number of applications have been projected for clay minerals; among others, their use as adsorbents of pollutants in order to reduce their environmental impact [3]. The interest in clay minerals has grown as the development of nanoscience and nanotechnology has progressed, due to their nano-sized layers and interlayer space [4–6].

Expandable clay minerals (i.e., smectites) have a marked hydrophilic character caused by the strong hydration of the inorganic counter ions present in the interlayer space. Indeed, they are rarely good adsorbents for hydrophobic organic compounds [7–10]. Nevertheless, the modification of the nature of the clay mineral surface from hydrophilic to hydrophobic through ion-exchange reactions replacing the inorganic cation with an organic cation can dramatically alter the affinity of smectites toward hydrophobic organic compounds. The resulting so-called organo-clays have been extensively proposed as adsorbents for poorly water soluble, highly hydrophobic compounds [3,11–15].

Alkylammonium-exchanged smectites have been the most common organo-clays proposed for adsorption of pesticides [3,16]. Celis et al. [17] found that the adsorption of the neutral fungicide triadimefon reached values higher than 90% after the modification of SAz-1 montmorillonite with hexadecyltrimethylammonium (HDTMA) monomeric cations, and a similar behavior was observed for neutral phenylureas pesticides [18,19]. Noticeable increases in adsorption of SAz-1 after its modification with HDTMA cations have also been reported for acidic pesticides, such as 2,4-D [13], imazamox [20], bentazone and dicamba [21], picloram [22] and MCPA [23,24]. However, several studies have pointed out that quaternary

alkylammonium ions such as HDTMA may have undesirable toxicological properties which may limit their usefulness for environmental applications. Several studies reported antimicrobial properties for this type of organo-clays, which can thus be toxic for natural xenobiotic degraders and hinder natural attenuation of pollutants in the environment [25,26]. Hence, new strategies to circumvent the limitations of traditional alkylammonium-modified clay minerals are needed. Alternative methods involve, for instance, preparation of clay-organic nanohybrid or nanocomposite materials using more friendly organic cations, capable of reducing the impact of the adsorbent once it is incorporated into natural environments for practical applications [18,24,27–30].

It is well-known that the leading mechanism in the adsorption of organic solutes by organo-clays will depend, for a given clay mineral, on the properties of the organic modifier and those of the selected solute [3,6]. The principal mechanism for the adsorption of organic pollutants on the traditional HDTMA-modified Arizona montmorillonite (SA-HDTMA) is the solute partitioning into the paraffinic-like organic phase formed by the vertical arrangement of HDTMA cations in the interlayer space of the clay mineral, which provides an excellent medium for the adsorption of hydrophobic organic compounds [11,31–33]. In the interaction of SA-HDTMA with anionic pesticides, including those of the phenoxyacetic group, polar interactions have also been proposed, in addition to hydrophobic interactions, as long as free polar space exists between alkylammonium groups in the organo-clay interlayer to host the pesticide [13,20,34–36].

In a preceding work, we found that the modification of SAz-1 Arizona montmorillonite with the cationic polymer hexadimethrine rendered a nanocomposite which displayed an affinity for the anionic pesticide MCPA comparable to that of the traditional SA-HDTMA organo-clay [24]. Given that the full potential of clay-organic nanohybrid materials has not been achieved due to limited understanding of the interaction mechanisms between different target

compounds and the clay matrix [16], we aimed in this work at getting further insight into the interaction mechanisms governing the adsorption of a number of structurally different pesticides, as representatives of widely spread pollutants in the environment, and the novel hexadimethrine-montmorillonite (SA-HEXAD) nanohybrid material, comparing its behavior with that of the well-known SA-HDTMA organo-clay. For the purpose of this work, HDTMA and HEXAD are excellent models of monomeric versus polymeric alkylammonium-type modifiers lacking additional specific functional groups for the adsorption of pesticides. The specific objectives of this work were: i) a detailed and comparative characterization of the SA-HEXAD and SA-HDTMA systems, and ii) a comparative assessment of the adsorption of a suite of structurally different pesticides by SA-HEXAD and SA-HDTMA, to get further insight into the mechanisms governing the affinity of these nanohybrids for selected pesticides. The information reported in this paper should be useful for the implementation of the assayed materials in specific applications, such as the removal of pesticides from contaminated water, their immobilization in soil, or the preparation of slow release formulations.

2. Experimental

2.1 Montmorillonite, organic cations and pesticides

The reference Ca-rich Arizona montmorillonite (SAz-1) from the Source Clays Repository of the Clay Minerals Society (Purdue University, West Lafayette, IN), with CEC equal to 1200 mmol/kg, was used for the preparation of the organo-clays. The properties of SAz-1 montmorillonite have been reported elsewhere [37].

Hexadimethrine (HEXAD) bromide (purity > 95%) and hexadecyltrimethylammonium (HDTMA) chloride (purity \geq 98%) (Fig. S1) were purchased from Sigma-Aldrich.

Hexadimethrine is an agglutinant blood cell polycation employed as heparin-neutralizing in

pharmaceutical industry [38]. Hexadecyltrimethylammonium is a cationic surfactant which has been widely used, among other applications, for the preparation of organo-clays [3,39].

Selected analytical-grade (purity > 99.9%) pesticides (fluometuron, diuron, terbuthylazine, simazine, mecoprop, MCPA, and clopyralid) supplied by Sigma-Aldrich were used for adsorption experiments. The structures of the pesticides are shown in Fig. 1.

2.2. Preparation of SA-HEXAD and SA-HDTMA nanohybrids

Preparation of SA-HEXAD and SA-HDTMA was accomplished through a cation exchange reaction, following the procedures described in Celis et al. [24,40]. Briefly, raw SAz-1 was treated with an aqueous solution containing an amount of organic cation (HEXAD or HDTMA) equivalent to 100% of the cation exchange capacity (CEC) of the clay mineral. The suspensions were shaken for 24 h, centrifuged, and the resulting solid was washed three times with deionized water, freeze-dried, and stored at room temperature until used.

2.3. Characterization of the unmodified and modified-montmorillonite samples

The C and N contents of the unmodified and modified-montmorillonites samples were determined by the combustion method using a Perkin-Elmer, model 1106 elemental analyzer (Perkin-Elmer Corp., Norwalk, CT). The basal spacings (d_{001}) of oriented clay specimens were determined with a Siemens D-5000 diffractometer (Siemens, Stuttgart) with CuK_α radiation. A Jasco FT/IR 6300 spectrometer (Jasco Europe s.r.l.) provided with a diffuse reflectance accessory was employed to record the Fourier-transform infrared (FTIR) spectra.

Physisorption of N_2 at 77 K, using a Carlo Erba Sorptomatic 1900 (Fisons Instruments, Milan) gas adsorption analyzer, was used to obtain the specific surface area (SSA) by applying the BET method. Zeta potential distribution curves for SAz-1, SA-HEXAD and SA-HDTMA suspensions (1.4 mg mL^{-1}) were measured with a Zetasizer Nano ZS equipment (Malvern

Instrument). Z potential (ξ) values were obtained at the pH of the suspension, previously dipped into an ultra-sound bath to disperse aggregates before analysis. Finally, scanning electron microscopy (SEM) was used to get insight into the morphology of the samples using a Hitachi S5200 microscope.

2.4. Adsorption studies

Adsorption experiments were conducted to determine the performance of SA-HEXAD as an adsorbent of a number of structurally different pesticides and to compare its behavior with that of SA-HDTMA, particularly with regard to different adsorption mechanisms possibly involved.

2.4.1. Preliminary adsorption study

A preliminary adsorption study with seven different pesticides (Fig. 1) was performed at a single initial pesticide concentration of 1 mg L^{-1} , using the batch equilibration technique. Triplicate 20 mg of SAz-1, SA-HEXAD or SA-HDTMA were placed in glass centrifuge tubes lined with screw caps. Subsequently, the clay samples were equilibrated with 8 mL of separate aqueous solutions of each pesticide with an initial concentration $C_i = 1 \text{ mg L}^{-1}$ by shaking at $20 \pm 2^\circ\text{C}$ for 24 h. After equilibration, the suspensions were centrifuged and 4 mL of the supernatant solution was removed, filtered, and analyzed by high performance liquid chromatography (HPLC) to determine the pesticide equilibrium concentration in solution, C_e (mg L^{-1}). Triplicate initial pesticide solutions of pesticides without adsorbent were also shaken for 24 h and served as controls. The percentage of pesticide adsorbed (% Ads) was calculated as: $\% \text{ Ads} = [(C_i - C_e)/C_i] \times 100$.

The HPLC system used for the determination of the initial and equilibrium pesticide concentrations was a Waters 600E chromatograph coupled to a Water 996 diode-array

detector. External calibration with four standard solutions between 0.1 and 2 mg L⁻¹ was used in the calculations. Different analytical conditions, in terms of chromatographic column, mobile phase, flow rate, and detection wavelength were required to analyze each pesticide; this information is compiled in Table S1 of the Supplementary data.

2.4.2. Adsorption-desorption isotherms of mecoprop (MCP) on SA-HEXAD and SA-HDTMA

According to the adsorption displayed by the pesticides on the organo-clays, mecoprop (MCCP) was chosen as a probe in order to get deep insight into the molecular interaction mechanism between anionic pesticides and the nanocomposites. For this purpose, adsorption and desorption isotherms of MCP on SAz-1, SA-HEXAD and SA-HDTMA were obtained. Triplicate 20 mg of each adsorbent were placed in glass centrifuge tubes lined with screw caps. Subsequently, 8 mL of aqueous solutions of MCP with initial concentrations ranging between 0.1 and 2 mg L⁻¹ were added and the resulting suspensions were equilibrated by shaking at 20 ± 2 °C for 24 h. After equilibration, the suspensions were centrifuged and 4 mL of the supernatant solution were removed, filtered and analyzed by HPLC to determine the equilibrium concentration (C_e) of MCP. The amount of MCP adsorbed, C_s (mg kg⁻¹), was calculated from the difference between the initial and equilibrium solution concentrations.

The MCP adsorption isotherms on SA-HEXAD was fitted to the linearized form of five two-parameter models (Langmuir, Freundlich, Temkin, Flory-Huggins, and Dubinin-Radushkevich) [41] and the corresponding adsorption parameters were calculated.

Desorption isotherms were obtained immediately after adsorption from the highest initial concentration point of the adsorption isotherm (2 mg L⁻¹). The 4 mL of supernatant removed for the adsorption analysis were replaced with 4 mL of distilled water. After shaking at 20 ±

2°C for 24 h, the suspensions were centrifuged and the MCPP concentration was determined in the supernatant by HPLC. This desorption procedure was repeated three times.

2.4.3. Adsorption mechanism of MCPP on SA-HEXAD and SA-HDTMA

A separate experiment was also conducted to elucidate the mechanisms involved in the adsorption of MCPP by the tested organo-clays. The working hypothesis was to assume that if non-specific ionic interactions motivated the adsorption of MCPP on SA-HEXAD, the presence of other anions in solution would depress the adsorption of the pesticide. Thus, the influence of electrolyte (CaCl_2) concentration in solution on the adsorption of MCPP by SA-HEXAD and SA-HDTMA was appraised. Adsorption at single initial concentration of MCPP (1 mg L^{-1}) on the organo-clays was performed by the batch method in water, 0.01 M CaCl_2 and 0.1 M CaCl_2 as background solutions. The procedure used to determine the percentage of MCPP adsorbed was identical to that described in section 2.4.1.

3. Results and discussion

3.1. Characterization of the unmodified and modified montmorillonites

3.1.1. Elemental analysis

The C and N contents of the unmodified and modified montmorillonite samples were used to calculate the percentage of the CEC of SAz-1 compensated by organic cations. According to the elemental analysis, HDTMA readily compensated (101%) the whole CEC of SAz-1, whereas the amount of HEXAD present accounted for 85% of the CEC of the clay mineral. This may suggest some difficulties for the polymer HEXAD to be intercalated into the clay, most likely as a consequence of its larger size compared to HDTMA (Fig. S1). The amounts of organic modifier in SA-HEXAD and SA-HDTMA were in good agreement with the values reported by Celis et al. [24] for similar organo-clays.

3.1.2. X-ray diffraction

The XRD diagrams of SAz-1, SA-HEXAD and SA-HDTMA showed the classical patterns of montmorillonites, where d_{001} values depended on the cation existing in the interlayer space (Fig. 2). The basal spacing of the unmodified SAz-1 montmorillonite was 1.52 nm, similar to the value reported in earlier studies [31,42]. The spacing of 1.52 nm is characteristic of two layers of hydration water surrounding the Ca^{2+} ions in the interlayer space [2,30,43]. The modification of SAz-1 with HEXAD resulted in a well-defined diffraction peak at 1.40 nm. This value is in agreement with a monolayer arrangement of the organic polymer in the interlayer space of the clay mineral, as previously proposed by Celis et al. [24]. The decrease in the d_{001} value of SAz-1 upon modification with HEXAD indicated that the incorporation of the organic cation into the clay mineral interlayer led to reduced swelling of the clay mineral compared to the presence of hydrated Ca^{2+} as counter ions [24,28]. Nevertheless, the basal spacing of 1.40 nm obtained for SA-HEXAD was greater than the values obtained for horizontal monolayer arrangements of other alkylammonium-exchanged montmorillonites [30,44–46] where ammonium groups ($-\text{NH}_2^+$ or $-\text{NH}_3^+$) were keyed into the ditrigonal cavities of the layers and established strong hydrogen bonds with the surface oxygen atoms [43,47]. This may reflect the steric hindrance of the $-\text{N}(\text{CH}_3)_2^+$ groups of hexadimethrine (Fig. S1) to be keyed into the ditrigonal cavities, as observed for other quaternary ammonium cations [8,40,48]. On the other hand, the d_{001} value corresponding to SA-HDTMA was 2.25 nm (Fig. 2), which is characteristic of a paraffinic arrangement of the HDTMA cations in the interlayer region in this organo-clay [31,49].

3.1.3. FTIR study

The FTIR technique was used to ascertain the presence of the organic modifiers in the prepared organo-clays (Fig. 3). The spectrum of SAz-1 showed bands at 3610 and 3390 cm^{-1} in the hydroxyl stretching vibration region, $\nu(\text{OH})$, the former corresponding to the structural OH groups of montmorillonite, and the latter to O-H vibrations of hydration water. It also showed a band at 1630 cm^{-1} attributed to the O-H bending mode, $\delta(\text{OH})$, of water molecules, and a band at 980 cm^{-1} due to the representative Si-O-Si stretching mode in clay minerals [2]. After modification of the clay mineral with the organic cations, the band at 3610 cm^{-1} remained unshifted for both organo-clays, indicating that the organic cations did not trigger significant changes on the clay layers. However, upward shifting of the bands assigned to the $\nu(\text{OH})$ stretching and $\delta(\text{OH})$ bending modes of hydration water were registered for both SA-HEXAD (3430 cm^{-1} and 1640 cm^{-1}) and SA-HDTMA (3410 cm^{-1} and 1640 cm^{-1}) (Fig. 3). This indicated higher freedom for water molecules in the organo-clays than that in the starting material, because polar interactions of the residual water molecules with the organic cations were weaker than those between water molecules and Ca^{2+} ions present in the pristine material. In addition, the low intensity observed for these bands was a consequence of the less hydration degree of the organo-clays compared to the unmodified mineral [24,30], which is consistent with the decrease in d_{001} value observed for SA-HEXAD compared to the starting material, SAz-1 (Fig. 2).

A remarkable feature of the FT-IR spectra was that both organo-clays exhibited bands characteristic of symmetric and antisymmetric C-H stretching vibrations, at 2950 and 2870 cm^{-1} for SA-HEXAD and 2923 and 2851 cm^{-1} for SA-HDTMA [50]. The group of bands appearing between 1490 and 1420 cm^{-1} in SA-HEXAD and between 1487 and 1416 cm^{-1} in SA-HDTMA can be assigned to C-H deformation vibrations [50]. The position of these bands at lower wavenumbers for SA-HDTMA respect to SA-HEXAD can be an indication of closer packing of the $-\text{CH}_2-$ groups, i.e. higher density of the alkylammonium chains, in the interlayer

space of SA-HDTMA, where the vibration of $-\text{CH}_2-$ groups appears to be more hindered than in SA-HEXAD.

3.1.4. N_2 adsorption isotherms: Determination of BET surface area

The N_2 adsorption isotherms for the unmodified and modified-montmorillonites samples (Fig. S2) showed the typical shape for clay materials [43,51–54]. The adsorption isotherms for all samples were type II, according to the IUPAC classification. The inflection points observed in the curves indicated the stage at which monolayer coverage is completed and multilayer adsorption begins to occur. In addition, the large nitrogen uptake observed close to saturation pressure is assigned to the presence of mesopores [43,53]. The modification of SAz-1 with HEXAD and HDTMA resulted in different BET specific surface area values (S_{BET}), which can be related to the nature of the organic cations and their arrangement on the mineral surfaces (Fig. S2). According to the N_2 isotherms, the S_{BET} decreased gradually in the following order: SAz-1 ($80 \text{ m}^2 \text{ g}^{-1}$) > SA-HEXAD ($51 \text{ m}^2 \text{ g}^{-1}$) > SA-HDTMA ($11 \text{ m}^2 \text{ g}^{-1}$), similar to the behavior reported by Wang et al. [54] for untreated and HDTMA-treated SAz-1 montmorillonite. The decrease in the S_{BET} for smectites upon treatment with organic cations has previously been observed by other authors [53–55], who attributed this effect to the organic cations clogging the pores and restricting the diffusion of N_2 [56]. Accordingly, the lower surface area and less hysteresis showed by SA-HDTMA compared to SA-HEXAD may reflect a more efficient surface covering and pore filling by HDTMA compared to HEXAD. It should be kept in mind that N_2 adsorption is commonly considered as a measure of the external surface area and, as such, it should not be used for total specific surface area or as an indicator of the amount of chemically accessible internal surface area. Considering preceding works, N_2 is not a suitable adsorbate for materials having pores smaller than 0.5 nm [57].

3.1.5. Zeta potential

The zeta potential (ξ) distribution curves for SAz-1, SA-HEXAD, and SA-HDTMA in water suspension are shown in Fig. 4. The zeta potential distribution curves of SAz-1 and SA-HDTMA, with maximum values at -23.8 mV and -4.6 mV, respectively, were in good agreement with results previously published by other authors [58,59]. These negative values reflect the key role of the external surfaces of the clay mineral [60]. Bate and Burns [60] pointed out that the zeta potential for organoclays became less negative for longer chains in alkylammonium-modified montmorillonite, suggesting some interactions of the organic cations within the shear plane. In contrast, several maximums, predominantly located at positive values, were observed in the zeta potential distribution curve of SA-HEXAD (Fig. 4). It is worthy to highlight that positive values of zeta potential were reported by other authors for organoclays when the amount of organic cation present exceeded the CEC of the clay [60]. Bleiman and Mishaal [61] also obtained positive values of zeta potential upon montmorillonite modification with chitosan, a positively-charged polymer. Hexadimethrine is a macromolecule and, as proposed by Lagaly [62], it can be expected that its arrangement in the montmorillonite surface would be governed by the distribution of charges in both the polymer and the clay [62]. Due to the heterogeneity of the charge distribution of clay mineral surfaces, it is likely that the polymer interacted with the clay surface forming loops and/or exposing unbalanced positive charges outside the sheets (Fig. 5) in such a way that not all $-\text{N}(\text{CH}_3)_2^+$ groups present in HEXAD directly interacted with the clay surface to compensate the layer charge of SAz-1 [62]. This would explain the positive zeta potential values observed in Fig. 4.

3.1.6. Scanning electron microscopy (SEM)

No great morphological changes were observed among samples when SAz-1, SA-HEXAD and SA-HDTMA were visualized at the micrometer scale by SEM (Fig. S3). This fact suggested either “functional” character of the nanohybrids, due to their different surface properties at the molecular scale, or that morphological differences primarily occurred at the nanometer scale, so that they could only have been seen at higher magnifications. It is well documented that the final morphology of organo-clays is conditioned by the nature and packing of the organic cation [26]. The unmodified SAz-1 montmorillonite showed aggregated and curled particles, whereas SA-HDTMA developed less aggregated morphology and flat plates and SA-HEXAD displayed an intermediate state between both (Fig. S3). It should be pointed out that for neither SA-HEXAD nor SA-HDTMA the amount of organic cation exceeded the CEC of the clay, and morphological changes at the micrometer scale have been reported mainly for organo-clays in which the amount of organic cation present exceeded the CEC of the clay mineral. In such cases, the structure became more regularly stacked [53] or montmorillonite adopted the shape of the organic modifier, as observed for SWy-2 montmorillonite modified with the cationic polymer chitosan [27].

3.2. Pesticide adsorption study on the organo-clays

3.2.1. Adsorption of pesticides on unmodified and modified montmorillonite at single initial concentration

The percentage of each pesticide adsorbed on unmodified and HEXAD- and HDTMA-modified SAz-1 montmorillonite is compiled in Table 1. It is important to note that at the pH of the equilibrated suspensions during the adsorption experiment ($\text{pH} > 6$), fluometuron, diuron, terbuthylazine and simazine existed as neutral species, whereas MCPP, MCPA and clopyralid (with $\text{pK}_a < 4$) existed mainly as anionic species. The original SAz-1 montmorillonite displayed very little affinity for all assayed pesticides (adsorption percentage $< 5\%$), but its

modification with HEXAD and HDTMA yielded organo-clays with greater affinity for selected pesticides (Table 1). The adsorptive behavior of the organo-clays depended on the properties of both the organic modifier and the considered pesticide. Thus, SA-HDTMA displayed high affinity for all pesticides (adsorption percentage > 70%) except simazine (Table 1), most likely due to its paraffinic structure which favors hydrophobic interactions with organic compounds [24,31,48]. However, SA-HEXAD displayed good adsorption of anionic pesticides only (i.e., mecoprop, clopyralid, and MCPA), for which adsorption percentages ranged between 50 and 75%. This fact is in agreement with the maximums located at positive values of the zeta potential value registered for this organo-clay (Fig. 4) and also with the hypothesis that the polymer would be bound to the clay surface exposing some $-N(CH_3)_2^+$ groups not directly interacting with the clay surface (Fig. 5), because these groups would act as adsorption sites for anionic pesticides. On the basis of its high adsorption on both nanohybrids, MCPP was selected for subsequent experiments designed to get further insight into the mechanisms governing the adsorption of anionic pesticides on SA-HEXAD and SA-HDTMA.

3.2.2. Adsorption-desorption isotherm of MCPP on SA-HDTMA and SA-HEXAD

Adsorption-desorption isotherms of MCPP on SA-HEXAD and SA-HDTMA are shown in Fig. 6. Since most of the pesticide present in the solution was uptaken by SA-HDTMA, only the adsorption isotherms for SA-HEXAD could be fitted to the two-parameter models explored in this work (Table 2). Among the different models tested, the Freundlich equation led to the best fitting of the MCPP adsorption data on SA-HEXAD ($R^2 = 0.999$).

The different adsorption behavior of MCPP on SA-HEXAD and SA-HDTMA was probably due to the distinct arrangement of the organic modifiers in the interlayer space of the clay [11]. Based on its shape, and supported by the obtained Freundlich N_f value of 1.22 ± 0.02 (Table S2), the adsorption isotherm of MCPP on SA-HEXAD was S-type according to the Giles et al.

[63] classification, similar to the isotherms obtained for the pesticide MCPA on the same organo-clay [23,24]. S-type isotherms are often related to competition between water molecules or ionic species in solution and the organic compound for adsorption sites and/or strong intermolecular interaction within the adsorbed layer of organic compound [63,64]. Hence, these results, together with zeta potential measurements (Fig. 4), strongly indicate that hexadimethrine polymer provided excess of positive charge which would contribute to the affinity displayed by SA-HEXAD for MCPP. The pesticide would be adsorbed by ionic forces, and intermolecular attraction probably occurred between the hydrophobic moieties (phenyl rings) of adsorbed MCPP species to result in the observed S-type isotherm behavior.

As mentioned above, the high adsorption of MCPP exhibited by SA-HDTMA can be related to hydrophobic interactions between the pesticide and the adsorbent, allowed by the paraffinic structure of the interlayer of this organo-clay [11,45]. As previously proposed by Hermosín and Cornejo [36] for the anionic pesticide 2,4-D, the adsorption could have also involved polar interactions between the ammonium groups of the alkylammonium and the carboxylic group of MCPP.

It is meaningful that, according to the desorption isotherm, MCPP showed some resistance to be desorbed from SA-HEXAD (Fig. 6). This circumstance can also be considered as an indication that the adsorption of this pesticide was governed by ionic forces, as formerly reported for the desorption of other anionic pesticides from organo-clays where water was used as desorbing solution [13,27,35]. The desorption isotherm of MCPP from SA-HDTMA was poorly defined as a consequence of the great adsorption capacity of this organo-clay and the very low pesticide concentration remaining in solution after adsorption.

3.2.3. Confirming the adsorption mechanism of the pesticide MCPP on SA-HEXAD and SA-HDTMA

To confirm the above-proposed adsorption mechanisms, the extent of MCPP adsorption on SA-HEXAD and SA-HDTMA at different background electrolyte (CaCl_2) concentrations was measured (Fig. 7). Our hypothesis was that if non-specific ionic interactions governed the adsorption of MCPP on SA-HEXAD and hydrophobic interactions governed its adsorption on SA-HDTMA, then high concentrations of a competing anion (Cl^-) would highly depress adsorption of MCPP on SA-HEXAD but not on SA-HDTMA. As expected, the adsorption of MCPP on SA-HEXAD was suppressed in 0.01 and 0.1 M CaCl_2 (Fig. 7), whereas an almost negligible effect was observed for SA-HDTMA. Since the adsorption of MCPP was reduced, the formation of Ca-MCPP complexes can be ruled out as a consequence of the presence of CaCl_2 , as it was reported for the adsorption of this pesticide on α -alumina and calcite [65]. In summary, the striking differences found in the adsorption behavior of SA-HEXAD and SA-HDTMA can be explained by different adsorption driving forces resulting from the structure of each organo-clay. Electrostatic interactions of anionic pesticides, such as MCPP, with positively charged sites at the surface, i.e. $-\text{N}(\text{CH}_3)_2^+$ groups not directly involved in the interaction with the clay, is proposed for SA-HEXAD. In contrast, hydrophobic interactions with the hydrophobic environment associated to the paraffinic structure of SA-HDTMA should be the main mechanism governing the adsorption of both neutral and anionic pesticides by this organo-clay. Nevertheless, polar/ionic interactions could have also slightly contributed to the adsorption of the anionic pesticides on SA-HDTMA, as indicated by the slight decrease in adsorption of MCPP observed in Fig. 7 at higher CaCl_2 concentration [13,66].

4. Conclusions

The study developed in this work shows that the cationic polymer hexadimethrine readily intercalates into SAz-1 Arizona montmorillonite with arrangement of the polycation in monolayers to yield a d_{001} value of 1.4 nm. The polymer also partially covers the external

surface of the clay exposing some of their $-N(CH_3)_2^+$ groups outside the interlayers of SAz-1, thus providing the resultant organo-clay with anion exchange properties. Comparative adsorption studies with the traditional HDTMA-modified Arizona montmorillonite (SA-HDTMA) showed that the extent of adsorption of pesticides on both organo-clays was conditioned by the arrangement of the organic cation on the clay surfaces. The paraffinic structure of SA-HDTMA led to high adsorption of all tested pesticides, mainly by pesticide-adsorbent hydrophobic interactions. In contrast, SA-HEXAD showed good adsorption of anionic pesticides only, with evidence that the driving forces for adsorption were ionic interactions. Therefore, we obtained a new nanocomposite based on hexadimethrine polymer modified-montmorillonite with selective affinity for anionic pesticides, which could be potentially useful as an adsorbent in applications such as the removal of pesticides from contaminated water, their immobilization in soil, or the preparation of slow release formulations. However, on the basis of the expected desorption of the adsorbed pesticide in the presence of saline solutions, we believe that the adsorbent could be particularly useful in the preparation of clay-based formulations of anionic pesticides to control their release once incorporated into the environment.

Acknowledgments

This work has been financed the Spanish Ministry of Economy and Competitiveness (MINECO Project AGL2011-23779) and Junta de Andalucía (JA Projects P07-AGR-03077 and P11-AGR-7400). B. Gámiz also thanks Junta de Andalucía for her postdoc-contract linked to Project P07-AGR-03077.

References

- 417 [1] F. Bergaya, G. Lagaly, General Introduction: Clays, Clay Minerals, and Clay Science,
418 in: F. Bergaya, B. Theng, G. Lagaly (Eds.), *Handb. Clay Sci.*, Elsevier, Amsterdam,
419 2006: pp. 1–18.
- 420 [2] C.T. Johnston, Probing the nanoscale architecture of clay minerals, *Clay Miner.* 45
421 (2010) 245–279.
- 422 [3] J. Cornejo, R. Celis, I. Pavlovic, M.A. Ulibarri, Interactions of pesticides with clays and
423 layered double hydroxides: a review, *Clay Miner.* 43 (2008) 155–175.
- 424 [4] D.H. Park, S. Hwang, J.M. Oh, J.H. Yang, J.H. Choy, Polymer–inorganic
425 supramolecular nanohybrids for red, white, green, and blue applications, *Prog. Polym.*
426 *Sci.* 38 (2013) 1442–1486.
- 427 [5] D. Manikandan, R.V. Mangalaraja, R. Siddheswaran, R.E. Avila, S. Ananthakumar,
428 Fabrication of nanostructured clay–carbon nanotube hybrid nanofiller by chemical
429 vapour deposition, *Appl. Surf. Sci.* 258 (2012) 4460–4466.
- 430 [6] Z. Gu, M. Gao, Z. Luo, L. Lu, Y. Ye, Y. Liu, Bis-pyridinium dibromides modified
431 organo-bentonite for the removal of aniline from wastewater: A positive role of π – π
432 polar interaction, *Appl. Surf. Sci.* 290 (2014) 107–115.
- 433 [7] S.A. Boyd, C.T. Johnston, D.A. Laird, B.J. Teppen, Comprehensive study of organic
434 contaminant adsorption by clays: methodologies, mechanisms, and environmental
435 implications, in: B. Xing, N. Senesi, P.M. Huang (Eds.), *Biophys. Process. Anthropog.*
436 *Org. Compd. Environ. Syst.*, John Wiley & Sons, Inc, 2011: pp. 51–71.
- 437 [8] W.F. Jaynes, G.F. Vance, BTEX sorption by organo-clays: cosorptive enhancement and
438 equivalence of interlayer complexes, *Soil Sci. Soc. Am. J.* 60 (1996) 1742–1749..
- 439 [9] G. Lagaly, Pesticide–clay interactions and formulations, *Appl. Clay Sci.* 18 (2001) 205–
440 209.
- 441 [10] M. Mortland, Clay-organic interactions, *Adv. Agron.* 23 (1970) 75–117.
- 442 [11] S.A. Boyd, S. Shaobai, J.F. Lee, M. Mortland, Pentachlorophenol sorption by organo-
443 clays, *Clays Clay Miner.* 36 (1988) 125–130.
- 444 [12] L. Groisman, C. Rav-Acha, Z. Gerstl, U. Mingelgrin, Sorption of organic compounds of
445 varying hydrophobicities from water and industrial wastewater by long- and short-chain
446 organoclays, *Appl. Clay Sci.* 24 (2004) 159–166.
- 447 [13] M. Hermosin, J. Cornejo, Removing 2,4-D from water by organo-clays, *Chemosphere.*
448 24 (1992) 1493–1503.
- 449 [14] M. Mortland, S. Shaobai, S.A. Boyd, Clay-organic complexes as adsorbents for phenol
450 and chlorophenols, *Clays Clay Miner.* 34 (1986) 581–585.
- 451 [15] S. Nir, Y. El-Nahhal, T. Undabeytia, G. Rytwo, T. Polubesova, Y. Mishaël, U.
452 Rabinovitz, R. Rubin, Clays and pesticides, in: F. Bergaya, B. Theng, G. Lagaly (Eds.),
453 *Handb. Clay Sci.*, Elsevier, Amsterdam, 2006: pp. 677–691.

- [16] B. Sarkar, Y. Xi, M. Megharaj, G. Krishnamurti, M. Bowman, H. Rose, R. Naidu, Bioreactive Organoclay : A New Technology for Environmental Remediation, *Crit. Rev. Environ. Sci. Technol.* (2012) 37–41.
- [17] R. Celis, W.C. Koskinen, M. Hermosín, M.A. Ulibarri, J. Cornejo, Triadimefon interactions with organoclays and organohydrotalcites, *Soil Sci. Soc. Am. J.* 64 (2000) 840–847.
- [18] B. Gámiz, R. Celis, M.C. Hermosín, J. Cornejo, Organoclays as soil amendments to increase the efficacy and reduce the environmental impact of the herbicide fluometuron in agricultural soils, *J. Agric. Food Chem.* 58 (2010) 7893–7901.
- [19] C. Trigo, R. Celis, M.C. Hermosín, J. Cornejo, Organoclay-based formulations to reduce the environmental impact of the herbicide diuron in olive groves, *Soil Sci. Soc. Am. J.* 73 (2009) 1652–1657.
- [20] R. Celis, W.C. Koskinen, A.M. Cecchi, G.A. Bresnahan, M.J. Carrisoza, M.A. Ulibarri, I. Pavlovic, M.C. Hermosín, Sorption of the ionizable pesticide imazamox by organoclays and organohydrotalcites, *J. Environ. Sci. Heal. Part B.* 34 (1999) 929–941.
- [21] M.J. Carrizosa, W.C. Koskinen, M.C. Hermosín, Interactions of acidic herbicides bentazon and dicamba with organoclays, *Soil Sci. Soc. Am. J.* 68 (2004) 1863–1866.
- [22] R. Celis, M.C. Hermosín, L. Cornejo, M.J. Carrizosa, J. Cornejo, Clay-herbicide complexes to retard picloram leaching in soil, *Int. J. Environ. Anal. Chem.* 82 (2002) 503–517.
- [23] A. Cabrera, L. Cox, K.A. Spokas, R. Celis, M.C. Hermosín, J. Cornejo, W.C. Koskinen, Comparative sorption and leaching study of the herbicides fluometuron and 4-chloro-2-methylphenoxyacetic acid (MCPA) in a soil amended with biochars and other sorbents, *J. Agric. Food Chem.* 59 (2011) 12550–12560.
- [24] R. Celis, C. Trigo, G. Facenda, M.C. Hermosín, J. Cornejo, Selective modification of clay minerals for the adsorption of herbicides widely used in olive groves, *J. Agric. Food Chem.* 55 (2007) 6650–6658.
- [25] J. Nye, W. Guerin, S.A. Boyd, Heterotrophic activity of microorganisms in soils treated with quaternary ammonium compounds, *Environ. Sci. Technol.* 28 (1994) 944–951.
- [26] B. Sarkar, M. Megharaj, Y. Xi, G.S.R. Krishnamurti, R. Naidu, Sorption of quaternary ammonium compounds in soils: implications to the soil microbial activities, *J. Hazard. Mater.* 184 (2010) 448–456.
- [27] R. Celis, M.A. Adelino, M.C. Hermosín, J. Cornejo, Montmorillonite-chitosan bionanocomposites as adsorbents of the herbicide clopyralid in aqueous solution and soil/water suspensions, *J. Hazard. Mater.* 209-210 (2012) 67–76.
- [28] M. Cruz-Guzmán, R. Celis, M.C. Hermosín, J. Cornejo, Adsorption of the herbicide simazine by montmorillonite modified with natural organic cations, *Environ. Sci. Technol.* 38 (2004) 180–186.

- 492 [29] B. Gámiz, R. Celis, L. Cox, M.C. Hermosín, J. Cornejo, Effect of olive-mill waste
493 addition to soil on sorption, persistence, and mobility of herbicides used in
494 Mediterranean olive groves, *Sci. Total Environ.* 429 (2012) 292–299.
- 495 [30] B. Gámiz, R. Celis, M.C. Hermosín, J. Cornejo, C.T. Johnston, Preparation and
496 characterization of spermine-exchanged montmorillonite and interaction with the
497 herbicide fluometuron, *Appl. Clay Sci.* 58 (2012) 8–15.
- 498 [31] W.F. Jaynes, S.A. Boyd, Clay mineral type and organic compound sorption by
499 hexadecyltrimethylammonium-exchanged clays, *Soil Sci. Soc. Am. J.* 55 (1991) 43–48.
- 500 [32] M.G. Roberts, H. Li, B.J. Teppen, S.A. Boyd, Sorption of nitroaromatics by
501 ammonium- and organic ammonium-exchanged smectite: shifts from
502 adsorption/complexation to a partition-dominated process, *Clays Clay Miner.* 54 (2006)
503 426–434.
- 504 [33] M.E. Parolo, G.R. Pettinari, T.B. Musso, M.P. Sánchez-Izquierdo, L.G. Fernández,
505 Characterization of organo-modified bentonite sorbents: The effect of modification
506 conditions on adsorption performance, *Appl. Surf. Sci.* 320 (2014) 356–363.
- 507 [34] M.J. Carrizosa, M.C. Hermosín, W.C. Koskinen, J. Cornejo, Use of organosmectites to
508 reduce leaching losses of acidic herbicides, *Soil Sci. Soc. Am. J.* (2003) 511–517.
- 509 [35] M. Cruz-Guzmán, R. Celis, M.C. Hermosín, W.C. Koskinen, J. Cornejo, Adsorption of
510 pesticides from water by functionalized organobentonites, *J. Agric. Food Chem.* 53
511 (2005) 7502–7511.
- 512 [36] M. Hermosín, J. Cornejo, Binding mechanism of 2,4-D from water by organo-clays, *J.*
513 *Environ. Qual.* 22 (1993) 325–331.
- 514 [37] C. Wang, Y. Ding, B.J. Teppen, S.A. Boyd, C. Song, H. Li, Role of interlayer hydration
515 in lincomycin sorption by smectite clays, *Environ. Sci. Technol.* 43 (2009) 6171–6176.
- 516 [38] M. Kikura, M. Lee, J. Levy, Heparin neutralization with methylene blue,
517 hexadimethrine, or vancomycin after cardiopulmonary bypass, *Anesth Analg.* 83 (1996)
518 223–227.
- 519 [39] N.H. Wang, S.L. Lo, Preparation, characterization and adsorption performance of
520 cetyltrimethylammonium modified birnessite, *Appl. Surf. Sci.* 299 (2014) 123–130.
- 521 [40] R. Celis, M.C. Hermosín, M.J. Carrizosa, J. Cornejo, Inorganic and organic clays as
522 carriers for controlled release of the herbicide hexazinone, *J. Agric. Food Chem.* 50
523 (2002) 2324–2330.
- 524 [41] K.Y. Foo, B.H. Hameed, Insights into the modeling of adsorption isotherm systems,
525 156 (2010) 2–10.
- 526 [42] C.J. Wang, Z. Li, W.T. Jiang, J.S. Jean, C.C. Liu, Cation exchange interaction between
527 antibiotic ciprofloxacin and montmorillonite, *J. Hazard. Mater.* 183 (2010) 309–314.
- 528 [43] M. Gautier, F. Muller, L. Le Forestier, J.M. Beny, R. Guegan, NH₄-smectite:
529 Characterization, hydration properties and hydro mechanical behaviour, *Appl. Clay Sci.*
530 49 (2010) 247–254.

- 531 [44] J.W. Jordan, Organophilic bentonites. I. Swelling in organic liquids, *J. Phys. Chem.* 53
532 (1949) 294–306.
- 533 [45] G. Lagaly, Characterization of clays by organic compounds, *Clay Miner.* 16 (1981) 1–
534 21.
- 535 [46] J.M. Serratosa, J. Rausell-Colom, J. Sanz, Charge density and its distribution in
536 phyllosilicates: Effect on the arrangement and reactivity of adsorbed species, *J. Mol.*
537 *Catal.* 27 (1984) 225–234.
- 538 [47] C.T. Johnston, E. Tombácz, Surface chemistry of soil minerals, in: J. Dixon, D. Schulze
539 (Eds.), *Soil Mineral. with Environ. Appl.*, Book Serie, SSSA, Madison, 2002: pp. 37–
540 67.
- 541 [48] J. Brixie, S. Boyd, Treatment of contaminated soils with organoclays to reduce
542 leachable pentachlorophenol, *J. Environ. Qual.* 23 (1994) 1283–1290.
- 543 [49] G. Lagaly, Layer charge heterogeneity in vermiculites, *Clays Clay Miner.* 30 (1982)
544 215–222.
- 545 [50] D.A. Myrzakozha, T. Hasegawa, J. Nishijo, T. Imae, An infrared study of molecular
546 orientation and structure in one-layer Langmuir - Blodgett films of
547 octadecyldimethylamine oxide and dioctadecyldimethylammonium chloride :
548 Dependence of the structures of the Langmuir - Blodgett films on substrates, aging, and
549 pH of water subphase, *Langmuir.* 15 (1999) 6890–6896.
- 550 [51] R.M. Barrer, D.M. MacLeod, Intercalation and sorption by montmorillonite, *Trans.*
551 *Faraday Soc.* 50 (1954) 980–989.
- 552 [52] S.K. Gregg SJ, Adsorption surface area and porosity, 2nd ed., Academic Press, London,
553 1982.
- 554 [53] H. He, Q. Zhou, W.N. Martens, T.J. Klopogge, P. Yuan, Y. Xi, J. Zhu, R.L. Frost,
555 Microstructure of HDTMA⁺-modified montmorillonite and its influence on sorption
556 characteristics, *Clays Clay Miner.* 54 (2006) 689–696.
- 557 [54] C.C. Wang, L.C. Juang, C.K. Lee, T.C. Hsu, J.F. Lee, H.P. Chao, Effects of exchanged
558 surfactant cations on the pore structure and adsorption characteristics of
559 montmorillonite, *J. Colloid Interface Sci.* 280 (2004) 27–35.
- 560 [55] Y. Park, G.A. Ayoko, R.L. Frost, Characterisation of organoclays and adsorption of p-
561 nitrophenol: environmental application, *J. Colloid Interface Sci.* 360 (2011) 440–56.
- 562 [56] H. He, R.L. Frost, T. Bostrom, P. Yuan, L. Duong, D. Yang, Y. Xi, J.T. Klopogge,
563 Changes in the morphology of organoclays with HDTMA⁺ surfactant loading, *Appl.*
564 *Clay Sci.* 31 (2006) 262–271.
- 565 [57] H. de Jonge, M. Mittelmeijer-Hazeleger, Adsorption of CO₂ and N₂ on soil organic
566 matter: Nature of porosity, surface area, and diffusion mechanisms, *Environ. Sci.*
567 *Technol.* 30 (1996) 408–413.
- 568 [58] E. Tombácz, M. Szekeres, Surface charge heterogeneity of kaolinite in aqueous
569 suspension in comparison with montmorillonite, *Appl. Clay Sci.* 34 (2006) 105–124.

- [59] P. Zarzycki, P. Szabelski, W. Piasecki, Modelling of ζ -potential of the montmorillonite/electrolyte solution interface, *Appl. Surf. Sci.* 253 (2007) 5791–5796.
- [60] B. Bate, S.E. Burns, Effect of total organic carbon content and structure on the electrokinetic behavior of organoclay suspensions, *J. Colloid Interface Sci.* 343 (2010) 58–64.
- [61] N. Bleiman, Y.G. Mishael, Selenium removal from drinking water by adsorption to chitosan-clay composites and oxides: batch and columns tests, *J. Hazard. Mater.* 183 (2010) 590–595.
- [62] G. Lagaly, *Inorganic Layer Compounds*, *Naturwissenschaften*. 68 (1981) 82–88.
- [63] C.H. Giles, T.H. MacEwan, S.N. Nakhwa, D. Smith, Studies in Adsorption. Part XI. A System of classification of solution adsorption isotherms, and its use in diagnosis of adsorption mechanism in measurement of specific surface area in solids, *J. Chem. Soc.* 846 (1960) 3973–3993.
- [64] R. Celis, M.C. Hermosin, L. Cox, J. Cornejo, Sorption of 2, 4-dichlorophenoxyacetic acid by model particles simulating naturally occurring soil colloids, *Environ. Sci. Technol.* 33 (1999) 1200–1206.
- [65] L. Clausen, I. Fabricius, L. Madsen, Adsorption of pesticides onto quartz, calcite, kaolinite, and alpha-alumina, *J. Environ. Qual.* 30 (2000) 846–57.
- [66] M.J. Carrizosa, W.C. Koskinen, M.C. Hermosin, J. Cornejo, Dicamba adsorption–desorption on organoclays, *Appl. Clay Sci.* 18 (2001) 223–231.

FIGURE CAPTIONS

Fig. 1. Structure of the pesticides used in this work.

Fig. 2. X-ray diffraction patterns of SAz-1, SA-HEXAD and SA-HDTMA.

Fig. 3. Fourier-transform infrared spectra of SAz-1, SA-HEXAD and SA-HDTMA.

Fig. 4. Zeta potential distribution curves for SAz-1, SA-HEXAD and SA-HDTMA.

Fig. 5. Schematic representation of the arrangement of HEXAD on SAz-1 bound to the surface forming loops and leaving positive charges on the external surface of the clay. Adapted from Lagaly [62].

Fig. 6. Adsorption-desorption isotherms of MCPP on SA-HEXAD and SA-HDTMA.

Fig. 7. Effect of salt concentration on the adsorption of MCPP by SA-HEXAD and SA-HDTMA.

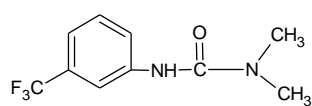
612 **Table 1**

613 Percentage of pesticide adsorbed on SAz-1, SA-HEXAD and SA-HDTMA

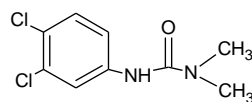
Pesticide	SAz-1	SA-HEXAD	SA-HDTMA
Fluometuron	< 5	< 5	90 ± 1 ^a
Diuron	< 5	< 5	95 ± 1
Terbuthylazine	< 5	< 5	77 ± 1
Simazine	< 5	< 5	28 ± 1
Mecoprop (MCP)	< 5	70 ± 2	95 ± 1
MCPA	< 5	54 ± 3	94 ± 1
Clopyralid	< 5	75 ± 3	84 ± 1

614 ^a value ± standard error

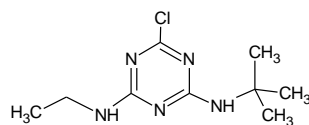
615



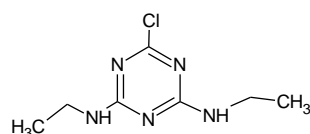
Fluometuron



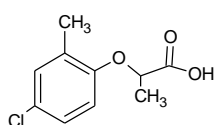
Diuron



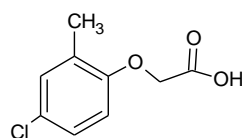
Terbutylazine



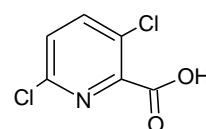
Simazine



Mecoprop



MCPA



Clopyralid

Fig. 1. Structure of the pesticides used in this work.

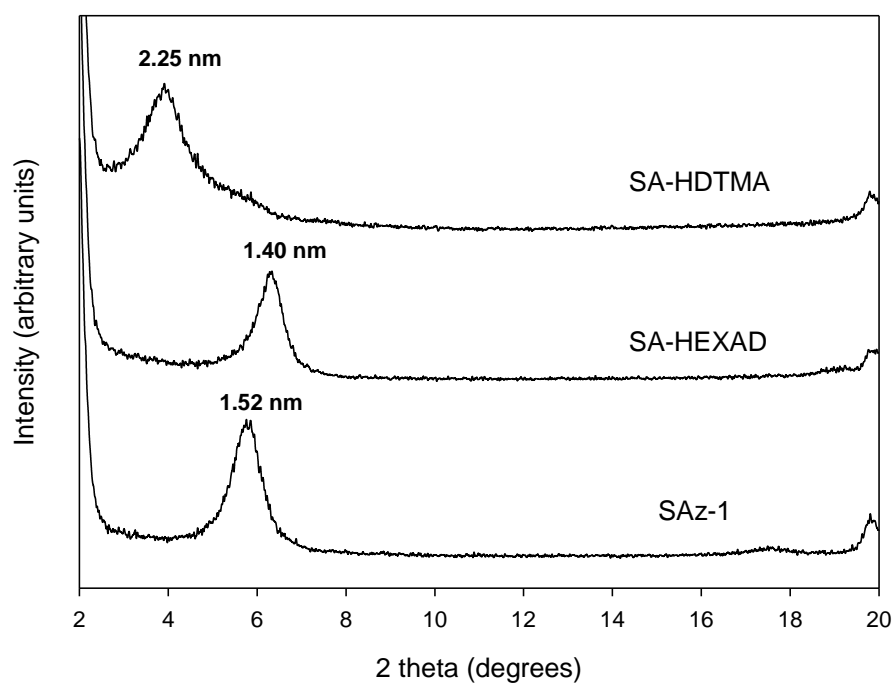


Fig. 2. X-ray diffraction patterns of SAz-1, SA-HEXAD and SA-HDTMA.

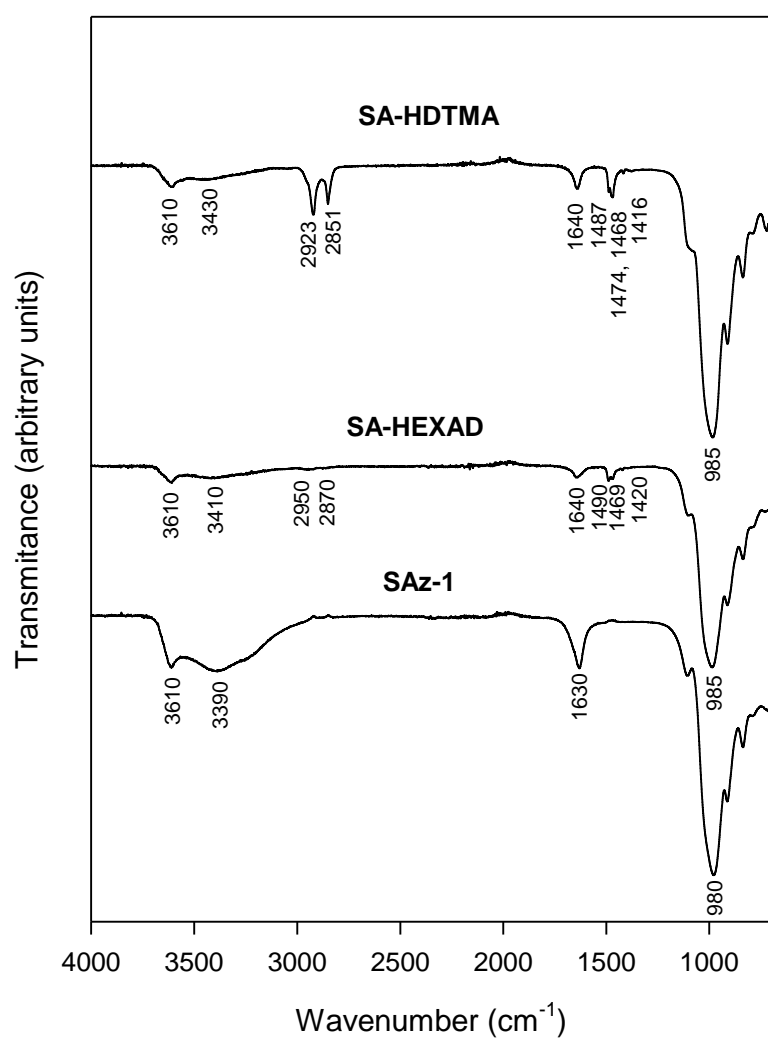


Fig. 3. Fourier-transform infrared spectra of SAz-1, SA-HEXAD and SA-HDTMA.

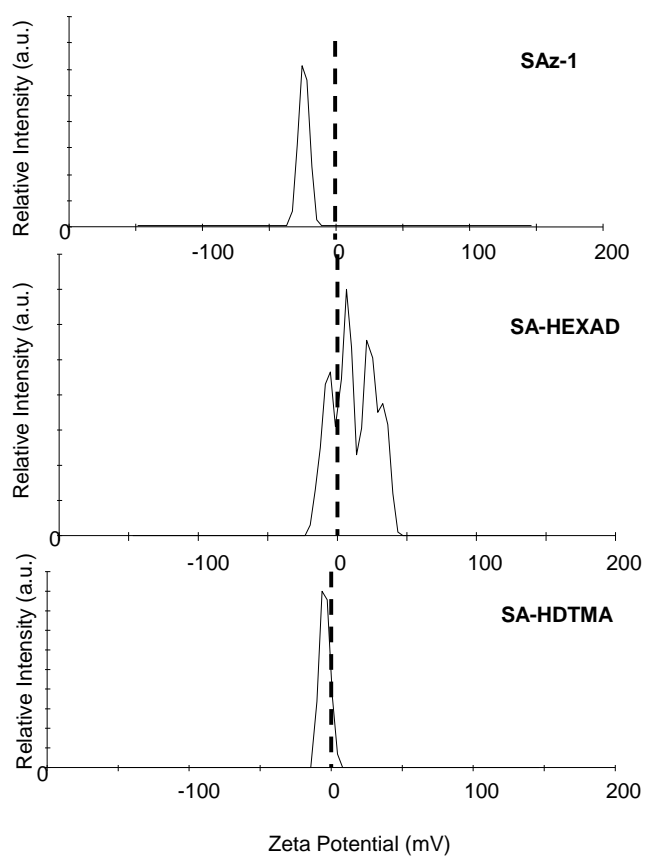


Fig. 4. Zeta potential distribution curves for SAz-1, SA-HEXAD and SA-HDTMA.

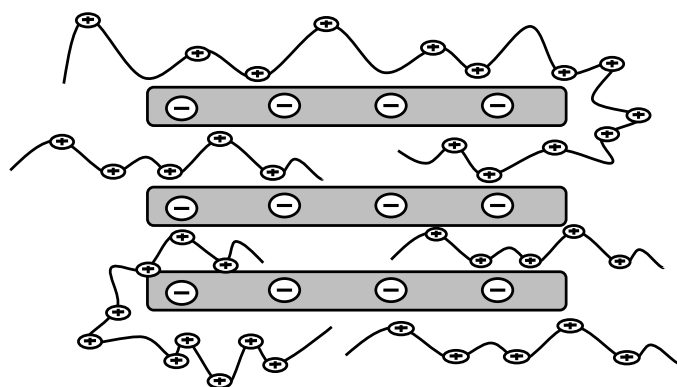


Figure 5. Schematic representation of the arrangement of HEXAD on SAz-1 bound to the surface forming loops and leaving positive charges on the external surface of the clay. Adapted from Lagaly [62].

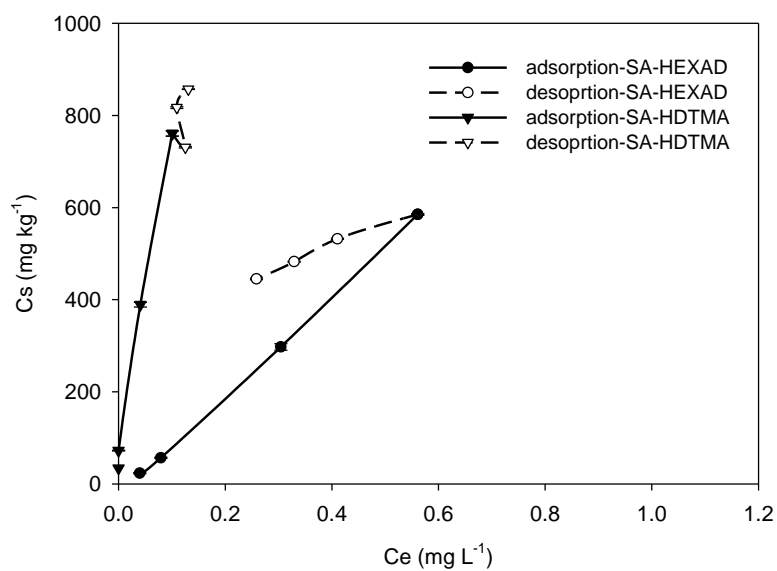


Fig. 6. Adsorption-desorption isotherms of MCP on SA-HEXAD and SA-HDTMA.

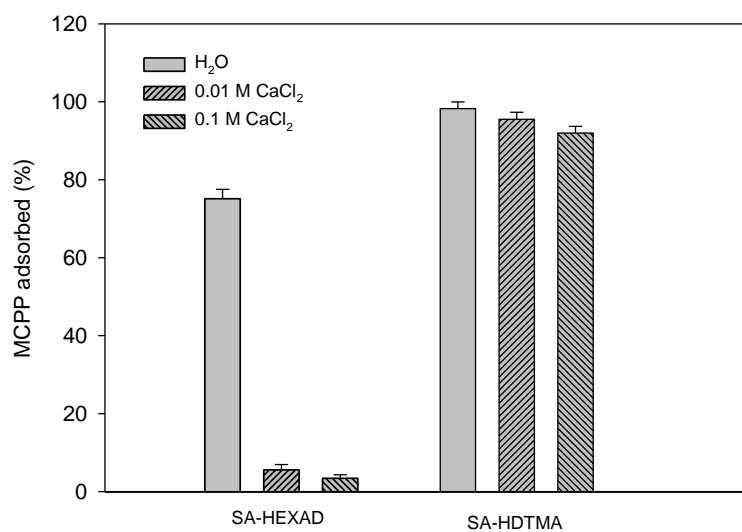


Fig. 7. Effect of salt concentration on the adsorption of MCPP by SA-HEXAD and SA-HDTMA.

Supplementary Data

Hexadimethrine-montmorillonite nanocomposite: characterization and application as a pesticide adsorbent

B. Gámiz*, M.C. Hermosín, J. Cornejo, R. Celis

Instituto de Recursos Naturales y Agrobiología de Sevilla (IRNAS), CSIC, Avenida Reina

Mercedes 10, P.O. Box 1052, 41080 Sevilla, Spain

*bgamiz@irnase.csic.es

Table S1Chromatographic conditions used for the analysis of the pesticides by HPLC^a.

Pesticide	Mobile phase ^b	Flow rate (mL/min)	Detection wavelength (nm)
Fluometuron	ACN:H ₂ O (40:60)	1	243
Diuron	ACN:H ₂ O (40:60)	1	250
Terbuthylazine	ACN:H ₂ O (50:50)	1	220
Simazine	ACN:H ₂ O (30:70)	1	230
Mecoprop (MCP)	MeOH:H ₃ PO ₄ dil. (70:30)	1	226
MCPA	MeOH:H ₃ PO ₄ dil. (60:40)	1	230
Clopyralid	ACN:H ₃ PO ₄ dil. (10:90)	0.7	222

^a In all cases, except for mecoprop, the chromatographic column was a Waters Nova-Pack C18 column of 150 mm length × 3.9 mm internal diameter. For MCP the column was a Supelcosil LC-18-DB of 150 mm length × 4.6 mm internal diameter. The sample injection volume was 25 µL.

^b ACN: acetonitrile; MeOH: methanol; H₃PO₄ dil.: diluted o-phosphoric acid (pH= 2).

758

759

Table S2

Linear forms and parameters of the isotherm models used in this work for adsorption of MCPP on SA-HEXAD.

Models	Linear form	Parameters	R ²
Freundlich ^a	$\log Cs = \log K_f + N_f \log Ce$	N _f = 1.22 K _f = 1224	0.999
Flory-Huggins ^b	$\log \frac{\theta}{C_o} = \log K_{FH} + n_{FH} \log(1 - \theta)$	K _{FH} = 4673 n _{FH} = 7.27	0.990
Dubinin-Radushkevich ^c	$\ln Cs = \ln q_s - K_{ad} \varepsilon^2$	q _s = 676 K _{ad} = 5.59 10 ⁻⁸	0.980
Temkin ^d	$Cs = \frac{RT}{b_T} \ln A_T + \frac{RT}{b_T} \ln Ce$	A _T = 21.40 b _T = 11.94	0.906
Langmuir ^e	$\frac{Ce}{Cs} = \frac{1}{CmL} + \frac{Ce}{Cm}$	C _m = -780 L = -0.809	0.797

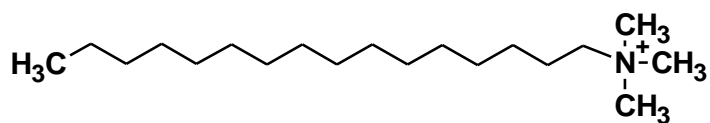
^a Ce: equilibrium concentration (mg L⁻¹); Cs: amount adsorbed (mg kg⁻¹); K_f(mg^{1-N_f} kg⁻¹ L^{N_f}) and N_f are the Freundlich parameters

^b $\theta = (1 - C_e/C_o)$; C_o: initial concentration (mg L⁻¹); K_{FH}: Flory-Huggins equilibrium constant (L mg⁻¹); n_{FH}: Flory-Huggins model exponent

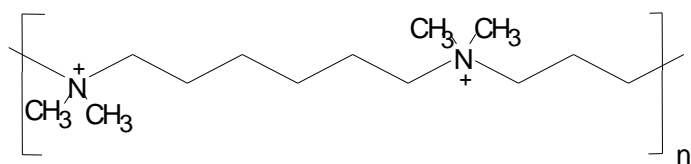
^c q_s is the theoretical adsorption capacity of the adsorbent (mg kg⁻¹); K_{ad}: constant related to the adsorption energy (mol² J⁻²); $\varepsilon = RT \ln [1 + (1/C_e)]$, R = 8.314 (J mol⁻¹ K⁻¹) and T temperature (K)

^d A_T: Temkin constant (L kg⁻¹); b_T: Temkin constant related to heat of adsorption (J mol⁻¹)

^e C_m: adsorbent monolayer capacity (mg kg⁻¹); L: Langmuir adsorption constant (L mg⁻¹)



Hexadecyltrimethylammonium (HDTMA)



Hexadimethrine (HEXAD)

Fig. S1. Structure of hexadecyltrimethylammonium (HDTMA) and the polymer hexadimethrine (HEXAD).

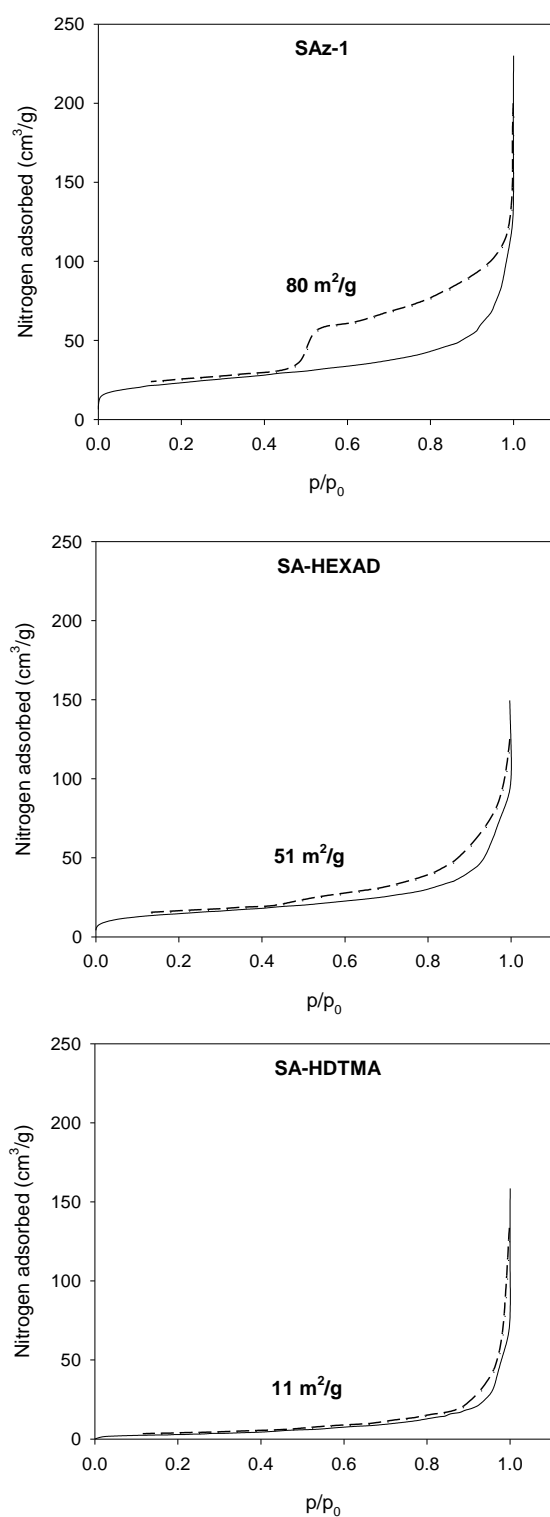


Fig. S2. N₂ adsorption isotherms and BET specific surface area of SAz-1, SA-HEXAD and SA-HDTMA.

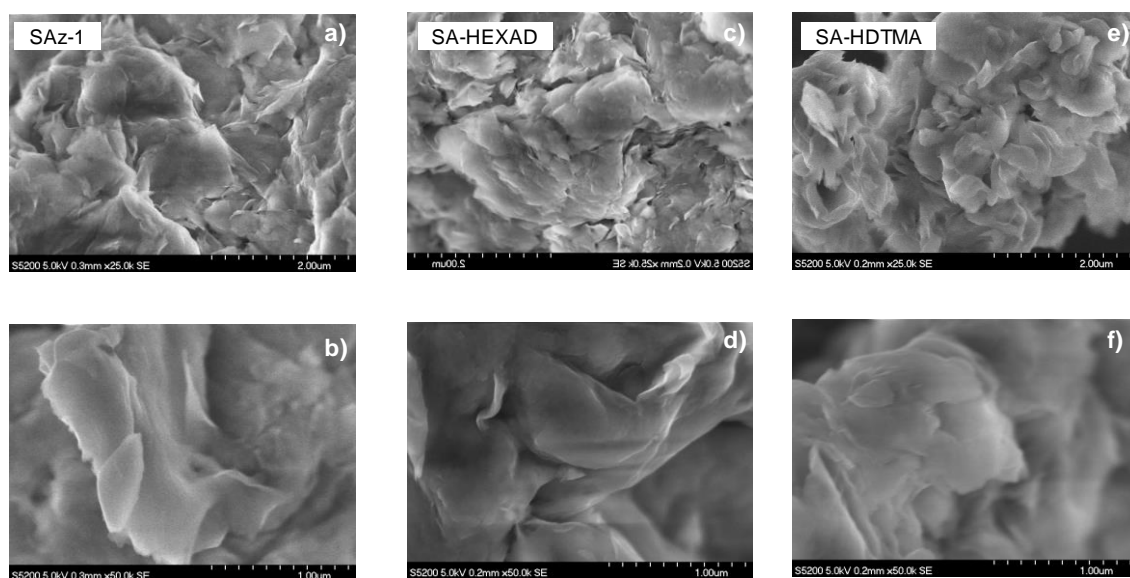


Fig. S3. SEM micrographs of SAz-1 (a and b), SA-HEXAD (c and d), and SA-HDTMA (e and f).